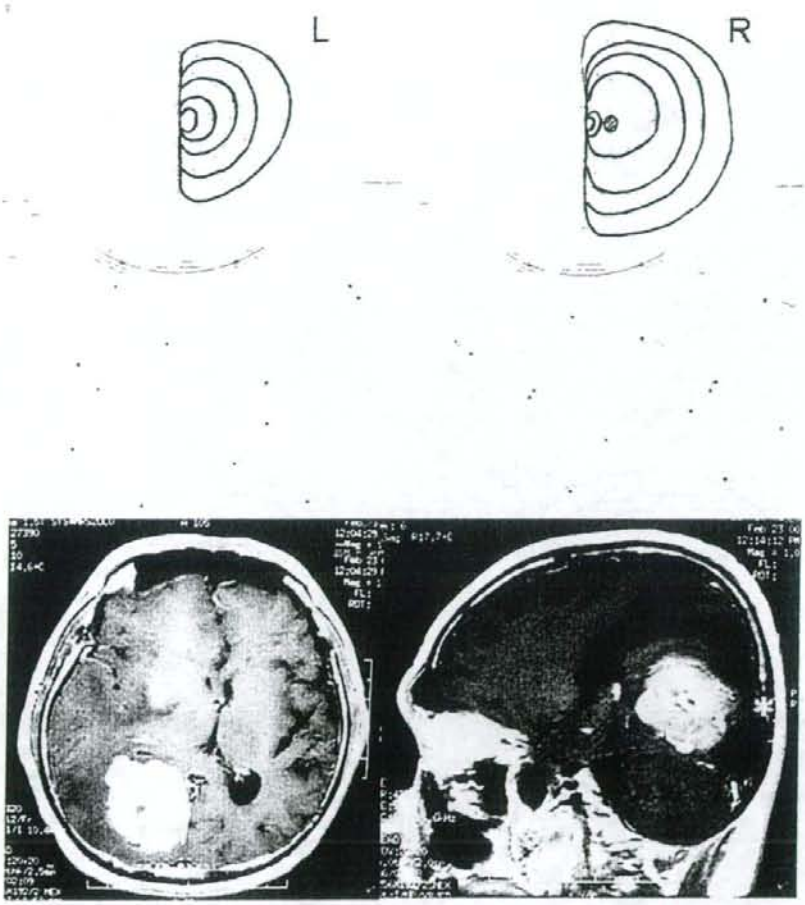

FIGURE 4. Findings in a 68-year-old-man (Case 8) who complained of visual loss in his left field and was found to have a glioma in the right occipital lobe. (Top) Goldmann perimetric fields showing a left homonymous hemianopsia. (Middle) The multifocal visual-evoked potentials (mfVEPs) are presented so that the average waveforms are seen in each of the quadrants where in the visual field each waveform originates. The mfVEPs have relatively good responses in the temporal fields of the left eye and the nasal fields of the right eye. (Bottom) An axial plane (left) and sagittal plane (right) of the magnetic resonance imaging (MRI) scan revealed a mass about 5 × 5 cm in the right occipital lobe, which was diagnosed as a glioma. Most of the lesion was primarily outside the primary visual cortex and in more distal areas.

normal limits in each quadrant in which the visual field was normal by conventional perimetry, and either the amplitude was reduced or the implicit time was delayed in the quadrants corresponding to the visual field deficits detected by perimetry. The visual field defects in these cases were due to a brain lesion outside the occipital cortex.

In contrast, the results of conventional perimetry and mfVEP topographic analysis in the other five cases were discordant. In these five patients, normal or only slightly reduced mfVEPs were recorded in the quadrants from which a subjective visual field deficit was detected. Interestingly in these cases, the site of the lesion was found in the occipital cortex in all five patients. Two of these cases (Cases 7 and 10) had a complete recovery of their visual field after the cause of the brain lesion was treated or in remission. In the five cases (Cases 1 through 5) in which the results from mfVEP were concordant with the subjective visual fields, there was no recovery of the visual fields determined by conventional perimetry.

• CASE 6: A 46-year-old man with a right homonymous hemianopsia from a meningioma. The ratios of the amplitude of the mfVEPs for SN/ST and IN/IT in the right eye were 0.618 and 1.792, respectively, whereas the normal ranges (mean ± 2 SD) were 0.311 to 1.763 and 0.155 to 1.85, respectively (Figure 2, Table 2). The ratios for SN/ST and IN/IT in the left eye were 1.630 and 0.485, respec-

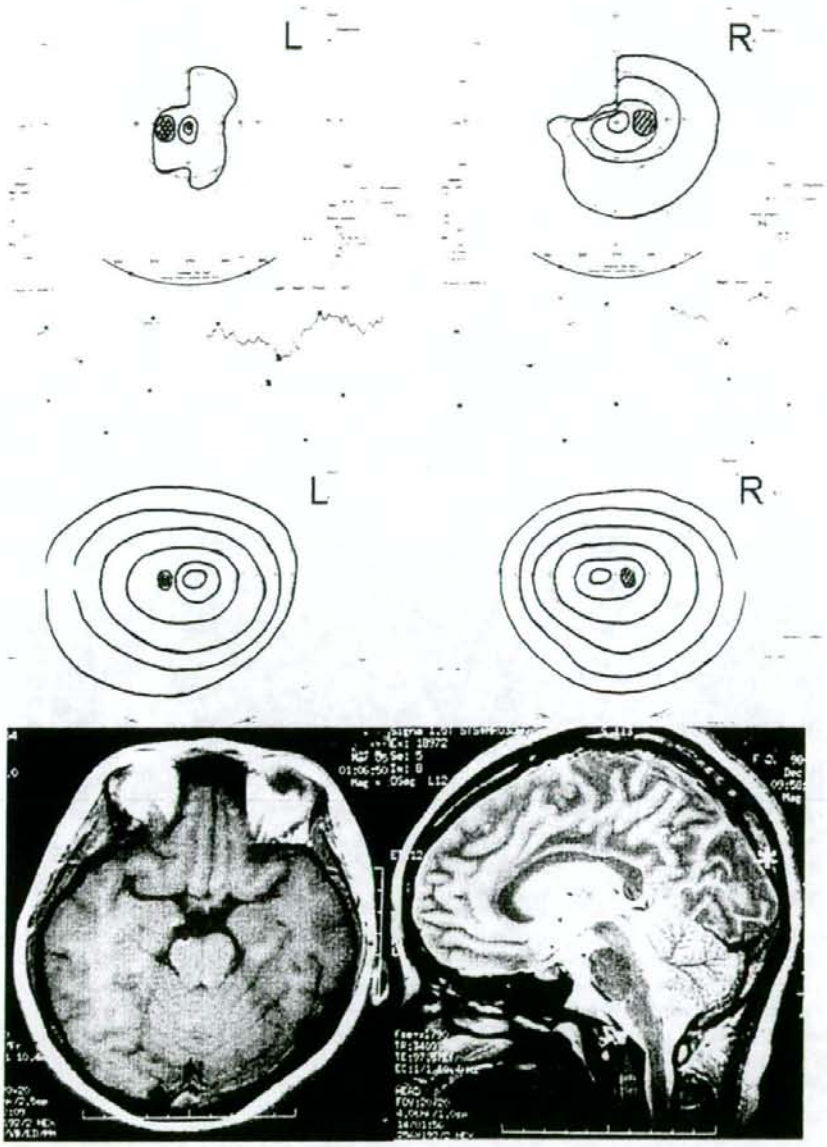

FIGURE 5. Findings in a 30-year-old-woman (Case 10) who underwent neurosurgery for subarachnoidal hemorrhage in the right occipital lobe resulting from an aneurysm of the posterior communicating artery. She complained of a visual field loss in the left field two months after surgery. (Top) Goldmann perimetric fields showing a left homonymous hemianopsia. (Second row) The multifocal visual evoked potentials (mfVEPs) are presented so that the average waveforms are seen in each of the quadrants where in the visual field each waveform originates. The mfVEPs demonstrated good responses in the nasal superior field of both eyes. (Third row) Three months later, the Goldmann fields demonstrate a complete recovery of the visual field. (Bottom right) An axial plane (left) and sagittal plane (right) of the magnetic resonance imaging (MRI) scan revealed neither particular edema nor infarction.

tively. All of these ratios were within the normal limits, suggesting that the mfVEPs were not altered in the temporal fields of the right eye and the nasal fields of the left eye. Therefore, his subjectively and objectively determined visual fields were discordant (Figure 2). His corrected visual acuity was 20/20 in both eyes, and Goldmann perimetry showed a right homonymous hemianopsia with foveal sparing. An MRI scan demonstrated a mass extending from the left parietal lobe to the occipital lobe, which was diagnosed as a meningioma.

• CASE 7: A 28-year-old man underwent surgery for an arteriovenous malformation in the right occipital lobe, and had homonymous hemianopsia postoperatively (Figure 3). The neurosurgeon referred the patient to our department for visual field examination. Examination revealed a corrected visual acuity of 20/20 in each eye, and Goldmann perimetry demonstrated a left homonymous hemianopsia. The ratios of the amplitudes of the mfVEPs for SN/ST and IN/IT in the right eye were 1.750 and 0.821, respectively (Table 2). The ratios for the left eye were 0.604 and 1.400, respectively (Table 2). All of the ratios were within the normal limits, suggesting that the mfVEPs were not altered the temporal fields of the left eye and the nasal fields of the right eye (i.e., a discordance).

Preoperative CT scan showed a nidus of about 2 × 2 cm on the right occipital lobe. CT scans seven days after the operation showed a low-density area that appeared to be postoperative edema. Goldmann perimetry showed a complete recovery of the visual fields three months after the operation.

• CASE 8: A 68-year-old man who had left homonymous hemianopsia from a glioma. The ratios of the amplitudes of the mfVEPs for SN/ST and IN/IT in the right eye were 1.130 and 0.612, respectively (Figure 4, Table 2). The same ratios for the left eye were 0.374 and 1.732, respectively. The ratios of the mfVEPs were within normal limits in the temporal field of the left eye and the nasal field of the right eye. His corrected visual acuity was 20/20 in each eye, and Goldmann perimetry showed a left homonymous hemianopsia. Therefore, his subjectively and objectively determined visual fields were concordant (Figure 4). An MRI scan revealed a mass about 5 × 5 cm in the right occipital lobe, which was diagnosed as a glioma.

• CASE 10: A 30-year-old woman who complained of a visual loss in the left field two months after neurosurgery for a subarachnoidal hemorrhage in the right occipital lobe resulting from an aneurysm in the posterior communicating artery. The neurosurgery caused a stenosis of the posterior cerebral artery. The ratios of the amplitudes of the mfVEPs for SN/ST and IN/IT in the right eye were 0.980 and 1.786, respectively. These findings indicate that the mfVEPs were not altered in the right eye even in the superior nasal visual field (Figure 5, Table 2). The ratios of the amplitude in the left eye were 0.803 and 0.462, respectively. The Goldmann visual field of the left eye showed reduced sensitivities in all the quadrants. The mfVEP amplitude for each quadrant was normal. She had a left homonymous hemianopsia with reduced sensitivities in the left eye postoperatively that showed discordance in both eyes (Figure 5). Her corrected visual acuity was 20/20 in each eye. Goldmann perimeter showed a left homonymous hemianopsia and concentric visual field deficit in the left eye. An MRI scan revealed neither edema nor infarction. Five months later, Goldmann perimetry demonstrated a complete recovery of the visual fields.

DISCUSSION

WE HAVE EVALUATED THE MFVEPS RECORDED WITH BIpolar occipital electrodes that straddled the inion and were elicited by a pseudorandom binary m sequence.[16] Our earlier results with the same stimulus and recording protocols showed that the summed mfVEPs in the four quadrants were highly concordant with the results of conventional subjective perimetry. Therefore, we concluded that this technique can be used to assess the visual field defects objectively in patients with diseases in the visual pathway.

However, as the number of such patients increased, we encountered some cases in which the mfVEPs were less impaired or even within normal limits in spite of visual field defects detected by conventional perimetry. We found that these discordant cases always had a lesion in the occipital area. However, the patients with homonymous hemianopsia from an occipital lesion did not always show such disagreement between subjective and objective visual fields.

The origin of human visual evoked potentials has been extensively investigated, and the evidence suggest that they originate from some part of the striate cortex or calcarine fissure.[14,15,26,32–34] Although the exact origin of the mfVEPs is still undetermined, they are believed to be mainly derived from area V1 of the striate cortex.[35–38] Therefore, mfVEPs and subjective visual field should be impaired from pathologic lesions in this area. If any part of the visual pathway before V1 is involved, the mfVEP recorded should be abnormal in the quadrants corresponding to the visual field defects, as seen in cases 1 and 2 in which chiasmal lesion led to bitemporal hemianopsia. In case 3, with a meningioma at the base of the skull, the mfVEPs were reduced in agreement with the homonymous left hemianopsia detected by Goldmann perimetry. This concordance can be reasonably explained by the postchiasmal damage of the visual pathway before V1.

However, localized damage of higher visual centers (e.g., V2/V3) can cause visual field defects when determined by perimetry but not by mfVEPs. We suggest that the discordance between the subjectively and objectively determined visual fields observed in the five cases was because the lesion was in the post-striate cortex. In the two cases (Cases 7 and 10) that had significant improvements of the visual field after a resolution of the brain lesion, we suggest that the postsurgical edema (Case 7) was the cause of the early visual field defect.

Klistner and associates recorded normal mfVEPs in patients with quadrantanopia that were consistent with an extrastriate lesion that was very congruous, complete, and respected the horizontal meridian. They stated that

mfVEPs are generated in the striate cortex (V1), and that topographic analysis of mfVEPs may be able to distinguish striate from extrastriate lesions.[17] Recently, a patient was reported with a congruous quadrantic defect and a loss of the fMRI signal in the corresponding extrastriate area, with normal signals in V1.[21]

Some investigators[1–5,39–44] have successfully recorded VEPs in cases with early compressive lesions of the optic tract, especially in the chiasmal or retrochiasmal regions. They reported that the VEP recordings were a sensitive and objective method for examining patients with visual field loss using full- or hemi-field stimulation or single or multichannel recordings. Flanagan and associates[40] reported that VEPs recorded with multichannel electrodes were useful and even more sensitive for detecting compressive lesions than subjective perimetry. In contrast, Maitland and associates[1] concluded that it was possible to lateralize the brain lesion, but not to predict the site of the lesion within the hemisphere. They also stated that VEP analysis is of only limited value in assessing patients with homonymous or bitemporal hemianopias.

On the basis of these findings, advanced mfVEP techniques with the dartboard pattern stimuli and recordings using bipolar occipital cross electrodes, as used in this study, enhanced the sensitivity of the VEPs in detecting postchiasmal optic nerve damage. Our findings clearly illustrate that the responses that were summed within each of the four quadrants were well-correlated with subjective perimetry in some patients. Moreover, this method was sensitive enough to detect visual field impairments even with macular sparing (Cases 7 and 10). Bradnam and associates[5] reported that a 90-minute check size used in their study, which is optimal for peripheral areas of the visual field, was minimally affected by central sparing of their VEP recordings. Although we are not certain whether full-field VEPs and mfVEPs are measuring the same thing, the dartboard pattern stimulus used in our study should stimulate the receptive fields optimally at each retinal eccentricity.[23] Therefore, they could improve the detection of incomplete hemi-field and quadrantic visual field defects and would be minimally affected by macular sparing. Further application of this technique on the large number of patients with visual field defects in the central area will be helpful in establishing whether this objective visual field testing can be used in patients with or without macular sparing.

In conclusion, there are some cases with lesions in the visual centers whose mfVEPs are not concordant with the subjective visual field. Two patients with this discordance had their hemianopsia recovered completely and three did not. We suggest that the mfVEPs originated from the primary area (area 17/V1). If the visual function arose from damage by a lesion in the higher visual centers, it is possible for the subjectively determined visual field to be dissociated from the mfVEPs. This means that damage of the visual pathway from the retina to the primary visual cortex (area 17/V1) would decrease the mfVEPs, but the damage of the higher visual cortex could lead to a discordance between the subjective visual field test and the mfVEPs. We suggest that the primary visual cortex was not affected severely in cases 7 and 10, and the transient tissue edema or circulation disturbance after neurosurgery was responsible for the subjectively determined visual field defects. In cases 6, 8, and 9, the brain tumor was not located in the primary visual cortex, and the mfVEPs could be recorded (V1). The mfVEPs even with conventional visual field defect can be interpreted to show that the primary visual cortex is not affected. In these cases, the visual field defect that is detected by conventional subjective visual field testing may recover. However, the recovery of visual field in the two cases may be associated with the cause of the visual field defect such as edema. Further investigation will be necessary to elucidate the mechanism of the recovery.[31]

THE AUTHORS INDICATE NO FINANCIAL SUPPORT OR FInancial conflict of interest. Involved in design and conduct of study (K.S., H.O.); involved in collection, management, analysis, and interpretation of the data (K.W., K.S., I.K., Y.M., Y.O., H.O.); and involved in preparation, review, and approval of the manuscript (K.W., K.S., I.K., Y.M., Y.O., H.O.).

REFERENCES

1. Maitland CG, Aminoff MJ, Kennard C, Hoyt WF. Evoked potentials in the evaluation of visual field defects due to chiasmal or retrochiasmal lesions. Neurology 1982;32:986–991.
2. Holder GE. Pattern visual evoked potential in patients with posteriorly situated space-occupying lesions. Doc Ophthalmol 1985;59:121–128.
3. Wildberger HG, van Lith GH, Wijngaarde R, Mak GT. Visually evoked cortical potentials in the evaluation of homonymous and bitemporal visual field defects. Br J Ophthalmol 1976;60:273–278.
4. Halliday AM, Halliday E, Kriss A, et al. The pattern-evoked potential in compression of the anterior visual pathways. Brain 1976;99:357–374.
5. Bradnam MS, Montgomery DM, Evans AL, et al. Objective detection of hemifield and quadrantic field defects by visual evoked cortical potentials. Br J Ophthalmol 1996;80:297–303.
6. Oguchi Y, Toyoda M. Vector analysis of pattern VEP. Doc Ophthalmol Proc Series 1981;27:239–245.
7. Kardon RH, Kirkali PA, Thompson HS. Automated pupil perimetry. Pupil field mapping in patients and normal subjects. Ophthalmology 1991;98:485–496.
8. Lehmann D, Skrandies W. Multichannel evoked potential fields show different properties of human upper and lower hemiretina systems. Exp Brain Res 1979;35:151–159.
9. Kiyosawa M, Mizuno K, Hatazawa J, et al. Metabolic imaging in hemianopsia using positron emission tomography with 18F-deoxyfluoroglucose. Am J Ophthalmol 1986;101:310–319.

10. Palmowski AM, Sutter EE, Bearse MA Jr, et al. Mapping of retinal function in diabetic retinopathy using the multifocal electroretinogram. Invest Ophthalmol Vis Sci 1997;38:2586–2596.
11. Bearse MA Jr, Sutter EE. Imaging localized retinal dysfunction with the multifocal electroretinogram. J Opt Soc Am A Opt Image Sci Vis 1996;13:634–640.
12. Kondo M, Miyake Y, Horiguchi M, et al. Clinical evaluation of multifocal electroretinogram. Invest Ophthalmol Vis Sci 1995;36:2146–2150.
13. Kretschmann U, Ruther K, Usui T, Zrenner E. ERG campimetry using a multi-input stimulation technique for mapping of retinal function in the central visual field. Ophthalmic Res 1996;28:303–311.
14. Baseler HA, Sutter EE, Klein SA, Carney T. The topography of visual evoked response properties across the visual field. Electroencephalogr Clin Neurophysiol 1994;90:65–81.
15. Klistorner AI, Graham SL, Grigg JR, Billson FA. Multifocal topographic visual evoked potential: improving objective detection of local visual field defects. Invest Ophthalmol Vis Sci 1998;39:937–950.
16. Betsuin Y, Mashima Y, Ohde H, et al. Clinical application of the multifocal VEPs. Curr Eye Res 2001;22:54–63.
17. Klistorner AI, Graham SL, Grigg J, Balachandran C. Objective perimetry using the multifocal visual evoked potential in central visual pathway lesions. Br J Ophthalmol 2005;89:739–44.
18. Seiple W, Holopigian K, Clemens C, et al. The multifocal visual evoked potential: an objective measure of visual fields? Vision Res 2005;45:1155–1163.
19. Graham SL, Klistorner AI, Goldberg I. Clinical application of objective perimetry using multifocal visual evoked potentials in glaucoma practice. Arch Ophthalmol 2005;123:729–739.
20. Miki A, Nakajima T, Fujita M, et al. Functional magnetic resonance imaging in homonymous hemianopsia. Am J Ophthalmol 1996;121:258–66.
21. Slotnick SD, Moo LR. Retinotopic mapping reveals extrastriate cortical basis of homonymous quadrantanopia. Neuroreport 2003;14:1209–1213.
22. Horton JC, Hoyt WF. The representation of the visual field in human striate cortex. A revision of the classic Holmes map. Arch Ophthalmol 1991;109:816–824.
23. Goldberg I, Graham SL, Klistorner AI. Multifocal objective perimetry in the detection of glaucomatous field loss. Am J Ophthalmol 2002;133:29–39.
24. Hood DC, Thienprasiddhi P, Greenstein VC, et al. Detecting early to mild glaucomatous damage: a comparison of the multifocal VEP and automated perimetry. Invest Ophthalmol Vis Sci 2004;45:492–498.
25. Klistorner AI, Graham SL. Multifocal pattern VEP perimetry: analysis of sectoral waveforms. Doc Ophthalmol 1999;98:183–196.
26. Baseler HA, Sutter EE. M and P components of the VEP and their visual field distribution. Vision Res 1997;37:675–690.
27. Cowey A, Rolls ET. Human cortical magnification factor and its relation to visual acuity. Exp Brain Res 1974;21:447–454.
28. Fox PT, Miezin FM, Allman JM, et al. Retinotopic organization of human visual cortex mapped with positron-emission tomography. J Neurosci 1987;7:913–922.
29. Whitteridgr D, Daniel PM. The visual system: neurophysiology and psychophysics. Berlin, Germany: Springer-Verlag; 1996:222–228.
30. Oguchi Y. Visual information processing and the mechanism of vision. Clinical application. Nippon Ganka Gakkai Zasshi 1998;102:850–875.
31. Graham SL, Klistorner A. Electrophysiology: a review of signal origins and applications to investigating glaucoma. Aust N Z J Ophthalmol 1998;26:71–85.
32. Jeffreys DA, Axford JG. Source locations of pattern-specific components of human visual evoked potentials. I. Component of striate cortical origin. Exp Brain Res 1972;16:1–21.
33. Onofrj M, Fulgente T, Thomas A, et al. Source model and scalp topography of pattern reversal visual evoked potentials to altitudinal stimuli suggest that infoldings of calcarine fissure are not part of VEP generators. Brain Topogr 1995;7:217–231.
34. Seki K, Nakasato N, Fujita S, et al. Neuromagnetic evidence that the P100 component of the pattern reversal visual evoked response originates in the bottom of the calcarine fissure. Electroencephalogr Clin Neurophysiol 1996;100:436–442.
35. Slotnick SD, Klein SA, Carney T, et al. Using multi-stimulus VEP source localization to obtain a retinotopic map of human primary visual cortex. Clin Neurophysiol 1999;110:1793–1800.
36. Hood DC, Greenstein VC. Multifocal VEP and ganglion cell damage: applications and limitations for the study of glaucoma. Prog Ret Eye Res 2001;22:201–251.
37. Fortune B, Hood DC. Conventional pattern-reversal VEPs are not equivalent to summed multifocal VEPs. Invest Ophthalmol Vis Sci 2003;44:1364–1375.
38. Zhang X, Hood DC. A principal component analysis of multifocal pattern reversal VEP. J Vision 2004;4:32–43.
39. Onofrj M, Bodis-Wollner I, Mylin L. Visual evoked potential diagnosis of field defects in patients with chiasmatic and retrochiasmatic lesions. J Neurol Neurosurg Psychiatry 1982;45:294–302.
40. Flanagan JG, Harding GF. Multi-channel visual evoked potentials in early compressive lesions of the chiasm. Doc Ophthalmol 1988;69:271–281.
41. Mashima Y, Oguchi Y. Visual evoked potential in the management of pituitary tumor during pregnancy. Doc Ophthalmol 1987;65:57–64.
42. Blumhardt LD, Barrett G, Halliday AM. The asymmetrical visual evoked potential to pattern reversal in one-half field and its significance for the analysis of visual field defects. Br J Ophthalmol 1977;61:454–461.
43. Holder GE. The effects of chiasmal compression on the pattern visual evoked potential. Electroencephalogr Clin Neurophysiol 1978;45:278–280.

Jpn J Ophthalmol 2006;50:554–556
DOI 10.1007/s10384-006-0373-6

BRIEF COMMUNICATION

Relaxation of Encircling Buckle Improved Choroidal Blood Flow in a Patient with Visual Field Defect Following Encircling Procedure

Itaru Kimura[1,2], Kei Shinoda[1,3], Tadahiko Eshita[1], Makoto Inoue[1], and Yukihiko Mashima[1]

[1]Department of Ophthalmology, Keio University School of Medicine, Tokyo, Japan;
[2]Laboratory of Clinical Epidemiology, National Institute of Sensory Organs, Tokyo, Japan;
[3]Laboratory of Visual Physiology, National Institute of Sensory Organs, Tokyo, Japan

Abstract

Background: We report a patient with a visual field defect after retinal reattachment by the encircling procedure for rhegmatogenous retinal detachment. We confirmed improved ocular blood flow after relaxation of the buckle.

Case: A 24-year-old woman with a visual field defect appearing after an encircling procedure for rhegmatogenous retinal detachment.

Observations: Before and after relaxing the encircling buckle, we measured tissue blood flow in the fundus of each eye of the patient using a Heidelberg retina flow meter. Preoperative measurements showed a reduction of blood flow at the disc rim in the diseased fundus, while retinal blood flow was not reduced ($P = 0.026$, disc rim area versus retinal area, one-factor analysis of variance, ANOVA). Indocyanine green angiography showed extensive peripheral filling delay. Electroretinography showed low a-wave and b-wave amplitudes, but normal oscillatory potential. The base value of the electro-oculogram was severely reduced in the right eye. The blood flow values after surgery indicated a significant improvement of blood flow ($P = 0.01$, one-factor ANOVA). No further progression in the visual field defect was observed, and visual acuity of the right eye improved from 0.8 to more than 1.0.

Conclusions: These results suggest that the choroidal circulation disturbance, which was found after the encircling procedure, had a plausible role in the development of the visual field defect. **Jpn J Ophthalmol** 2006;50:554–556 © Japanese Ophthalmological Society 2006

Key Words: choroidal blood flow, encircling procedure, rhegmatogenous retinal detachment, scanning laser Doppler flowmetry, visual field defect

Introduction

There have been various reports concerning an adverse effect on ocular circulation of the scleral buckling procedure.[1–4] Choroidal and retinal blood flow was significantly decreased in eyes of rabbits buckled with encircling elements.[1] Further clinical evidence, for example, a 40% decrease[2] in the blood flow velocity of the choroid–retina on the buckled side and an average blood flow rate 50% lower[3] through the major temporal retinal arteries in the surgically treated eye compared with that in the fellow eye after scleral buckling for rhegmatogenous retinal detachment (RRD), has been reported. Compression mechanisms were cited as the cause of the reduced choroidal blood flow following scleral buckling procedures. However, although retinal blood flow in the macular area was reported to be disturbed in RRD patients without macular involvement, it recovered to an almost normal level 1 month after successful scleral buckling procedures.[4]

Received: January 7, 2005 / Accepted: May 16, 2006
Correspondence and reprint requests to: Itaru Kimura, Department of Ophthalmology, Keio University School of Medicine, 35 Shinanomachi, Shinjuku-ku, Tokyo 160-8582, Japan
e-mail: kimura@sc.itc.keio.ac.jp

We present a case of visual field defect (VFD) after retinal reattachment by an encircling procedure (EC) for peripheral RRD.

Case Report

In February 1999, in another hospital, a 24-year-old woman underwent EC for inferotemporal RRD in association with atopic dermatitis in her right eye. Six months later, she noticed an inferior VFD in her right eye, which had not existed before. The patient was referred to our clinic. Best-corrected visual acuities were 0.8 OD, 1.0 OS, and intraocular pressure (IOP) was 14 mmHg OU. Ophthalmoscopy showed no recurrence of RRD but a high indentation of the encircling buckle. Neither quadrant swelling of the optic disc nor retinal vessel branch obstruction in the area corresponding to the VFD was observed. Goldmann perimeter showed a wedge-shaped inferior peripheral VFD expanding to around 10° of the central visual field in the right eye (Fig. 1a), while the left eye showed a normal visual field. Single-flash electroretinogram (ERG) showed low a-wave and b-wave amplitudes, but normal oscillatory potential in the right eye, whereas the response of the left eye was normal (Fig. 1b). In an electro-oculogram (EOG), the base value was severely reduced in the patient's affected eye (Fig. 1c).

Fluorescein angiography (FA) showed no remarkable abnormal findings, but indocyanine green angiography (IA) indicated an extensive peripheral filling delay.

Tissue blood flow was measured at four retinal areas in both eyes with a Heidelberg retina flow meter (HRF, Heidelberg Engineering, Heidelberg, Germany), including the superior and inferior disc rim areas and paramacular areas. Mean blood flow (MBF) in each area was obtained using an automatic full-field perfusion image analyzer[5] (version 3.3, Heidelberg Engineering, Table 1). The ratio of the MBF of the affected eye to that of the fellow eye (a/f ratio) was calculated for each area to minimize the interexamination variation.[6] The a/f ratios at the paramacular area were 1.04 and 1.45, superior and inferior, respectively; whereas the

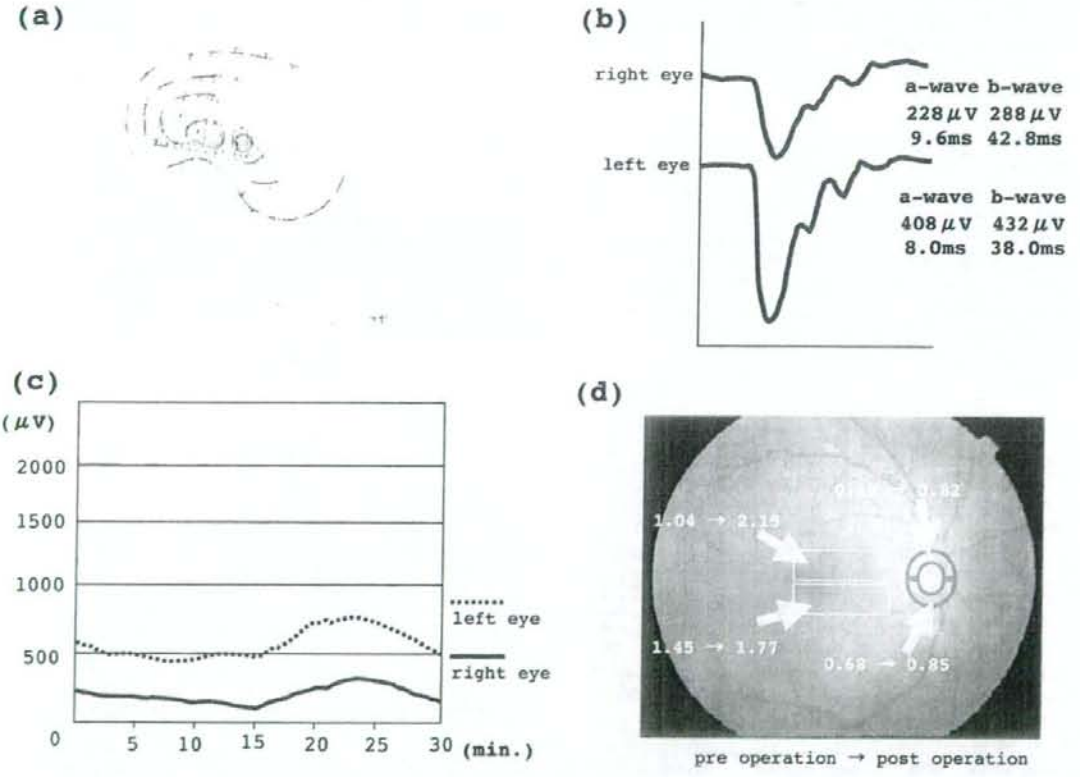

Figure 1. **a** Results of Goldmann perimetry 6 months after encircling procedure. **b** Single flash electroretinogram. Low amplitudes of a-wave in the right eye. **c** Electro-oculogram. Reduced base value in the right eye. Light peak/dark trough ratios were 2.142 in the right eye and 1.700 in the left eye. **d** Affected/fellow eye (a/f) ratio before buckle relaxation surgery and 6 weeks afterward. Preoperative measurements showed reduction of blood flow in disc rim of the diseased fundus ($P = 0.026$ for disc rim area versus retinal area). The mean ratio of each area indicated a significant improvement of blood flow after surgery ($P = 0.01$, one-factor analysis of variance).

Jpn J Ophthalmol
Vol 50: 554–556, 2006

Table 1. Mean blood flow values and a/f ratios by HRF at each measurement area

	Neuroretinal rim area						Paramacular area					
	Superior			Inferior			Superior			Inferior		
	a	f	a/f	a	f	a/f	a	f	a/f	a	f	a/f
Pre-op	138.9	349.9	0.40	229.4	336.1	0.68	255.0	245.9	1.04	235.5	162.3	1.45
Post-op	215.8	262.1	0.82	253.9	297.2	0.85	572.9	266.4	2.15	323.3	245.0	1.77

Values are expressed in arbitrary units.
HRF, Heidelberg retina flow meter; a, affected eye; f, fellow eye, Pre-op, preoperation; Post-op, postoperation; a, affected eye; f, fellow eye; a/f, affected eye/fellow eye ratio.

ratios at the disc rim area were 0.40 and 0.68, superior and inferior, respectively, which is highly suggestive of decreased blood flow at the disc rim ($P = 0.026$, disc rim area versus retinal area, Fig. 1d). Therefore, the association of the VFD with the compromised choroidal circulation was highly suspected. Considering the possibility of retinal redetachment, removal of the encircling buckle was postponed.

In February 2001, with the intention of improving circulation but keeping indentation, the EC buckle was cut off at one part. The silicone band had been buckled about 15 mm from the corneal limbus. The degree of retinal elevation caused by the buckle did not change ophthalmoscopically before and after relaxing the EC. Six weeks later, the a/f ratios were 2.15 and 1.77, superior and inferior, respectively, at the paramacular area, and 0.82 and 0.85, superior and inferior, respectively, at the disc rim area, showing a significant improvement of blood flow ($P = 0.01$, one-factor analysis of variance, Fig. 1d). ERG, EOG, and Goldmann perimetry showed no remarkable change. Visual acuity of the right eye had ranged from 0.5 to 0.9 before relaxation of the EC buckle, but after buckle relaxation, visual acuity improved to 1.0 or higher, and has been steadily maintained at this level since. No further progression of the visual field defect has been observed after 3 years of follow-up.

Discussion

The current case demonstrated reduced tissue blood flow at the disc rim area that improved after relaxation of the EC buckle. However, the tissue blood flow at the paramacular area was normal. Blood flow of the inner retina and nerve fiber layer of the disc are supplied by the central retinal artery or its branches, while blood flow in the prelaminar region adjacent to nerve fiber layer is supplied by branches of juxtapapillary choroidal vessels. Flow values at the disc rim obtained by HRF are considered to be a mixture of retinal and choroidal blood flow contributions because the depth of laser penetration is about 400 μm. Therefore, the laser scanning depth includes the nerve fiber layer and prelaminar regions.

The findings in this case suggest that EC predominantly disturbs choroidal circulation while leaving retinal circulation intact over the long term following EC. The findings of FA and IA support these results. An alternative explanation is that the macular microcirculation is less susceptible to the compression force of the buckle, which could persistently affect the blood flow in main ocular vessels. Investigation of the retinal and choroidal blood flow changes shortly after the EC procedure would be helpful to clarify these hypotheses.

The electrophysiological parameters, such as low a-wave and b-wave amplitudes but normal oscillatory potential in ERG, and the severely reduced base value of EOG in the affected eye, suggest that VFD after EC is caused by dysfunction of the outer retinal layer, mainly due to the disturbance of choroidal circulation, supporting the MBF measurements. The patient noticed her visual field defect 6 months after the EC procedure. We speculate that her visual field disturbance progressed gradually during this period.

Electrophysiological testing together with ocular blood flow measurement might be useful in some cases to understand the mechanism of such complications as VFD.

In this case, visual acuities improved from under 1.0 to 1.0 or higher after relaxing the EC buckle. This change was inferred to result from choroidal and retinal circulation improvement caused by relaxing of the EC buckle.

Because preservation of the scleral indentation was preferred, the EC buckle was relaxed. This simple procedure can be considered for improving choroidal circulation, especially in patients who are suffering from VFD after EC.

References

1. Diddie KR, Ernest JT. Uveal blood flow after 360° constriction in the rabbit. Arch Ophthalmol 1980;98:729–730.
2. Nagahara M, Tamaki Y, Araie M, Eguchi S. Effects of scleral buckling and encircling procedures on human optic nerve head and retinochoroidal circulation. Br J Ophthalmol 2000;84:31–36.
3. Ogasawara H, Feke GT, Yoshida A, Milbocker MT, Weiter JJ, McMeel JW. Retinal blood flow alterations associated with scleral buckling and encircling procedures. Br J Ophthalmol 1992;76:275–279.
4. Eshita T, Shinoda K, Kimura I, et al. Retinal blood flow in the macular area before and after scleral buckling procedures for rhegmatogenous retinal detachment without macular involvement. Jpn J Ophthalmol 2004;48:358–363.
5. Michelson G, Wezenbach J, Pal I, Harazny J. Automatic full field analysis of perfusion images gained by scanning laser Doppler flowmetry. Br J Ophthalmol 1998;82:1294–1300.
6. Kimura I, Shinoda K, Tanino T, Ohtake Y, Mashima Y, Oguchi Y. Scanning laser Doppler flowmeter study of retinal blood flow in macular area of healthy volunteers. Br J Ophthalmol 2003;87:1469–1473.

the evaluation for CTX to support early definitive therapy. Moreover the measurement of cholestanol levels when a subject is initially seen with presenile cataracts of questionable etiology could be a valuable clinical tool.

Alexandra Tészás, MD
Zoltán Pfund, MD
Éva Morava, MD, PhD
György Kosztolányi, MD, DSci
Erik Sistermans
Ron A. Wevers
Richard Kellermayer, MD, PhD

Correspondence: Dr Kellermayer Department of Medical Genetics and Child Development, University of Pécs, József A. u. 7, Pécs 7623, Hungary (richard.kellermayer@aok.pte.hu).

Financial Disclosure: None reported.

1. Tonius H, Arentz-Grastvedt B, Eriksson AW. Juvenile cataract with autosomal recessive inheritance: a study from the Aland Islands, Finland. *Acta Ophthalmol (Copenh)*. 1992;70:26-32.
2. Verrips A, van Engelen BG, Wevers RA, et al. Presence of diarrhea and absence of tendon xanthomas in patients with cerebrotendinous xanthomatosis. *Arch Neurol*. 2000;57:520-524.
3. Lorincz MT, Rainier S, Thomas D, Fink JK. Cerebrotendinous xanthomatosis: possible higher prevalence than previously recognized. *Arch Neurol*. 2005;62:1459-1463.
4. Batta AK, Salen G, Tint GS. Hydrophilic 7 beta-hydroxy bile acids, lovastatin, and cholestyramine are ineffective in the treatment of cerebrotendinous xanthomatosis. *Metabolism*. 2004;53:556-562.
5. van Heijst AF, Verrips A, Wevers RA, Cruysberg JR, Renier WO, Tolboom JJ. Treatment and follow-up of children with cerebrotendinous xanthomatosis. *Eur J Pediatr*. 1998;157:313-316.

Familial Retinal Arterial Tortuosity Associated With Tortuosity in Nail Bed Capillaries

Familial retinal arterial tortuosity (fRAT) is characterized by marked tortuosity of second- and third-order retinal arteries with normal first-order arteries and venous system. Patients have variable transient vision loss owing to retinal hemorrhages after minor stress or trauma. Prognosis is usually excellent. Whether there is systemic involvement is controversial. We report 3 cases of fRAT associated with a high degree of tortuosity of capillaries at nailfold capillaroscopy as an indication of systemic vascular pathology.

Report of Cases. *Case 1.* A woman was first seen at age 19 years because of blurred vision after a minor car accident. Best-corrected visual acuity (BCVA) was 0.9 OD and 0.8 OS. Ophthalmologic examination revealed marked tortuosity of second- and third-order retinal arteries and multiple intraretinal and preretinal hemorrhages in both eyes (**Figure 1**A). The patient was observed. Four weeks later, BCVA was fully restored in both eyes and the hemorrhages had almost resolved.

Five years later, the patient reported frequent episodes of migraine. Tortuosity of the retinal vessels and BCVA remained unchanged, but the macular reflex appeared duller, and mild thickening of the inner limiting membrane was noted in both eyes (Figure 1B). No hemorrhages were observed.

Seven years after she was first seen, the patient had decreased visual acuity of 0.4 OD and 0.8 OS. She was in her 18th week of pregnancy and had undergone amniocentesis 2 days previously. Fundus examination showed several preretinal, foveal hemorrhages in both eyes. Four weeks later, BCVA returned to 1.0 OU and hemorrhages had resolved.

Twelve years after she was first seen, the patient reported episodes of blurred vision once per year, usually following minor exercise. Best-corrected visual acuity had always fully recovered. At this ophthalmologic examination, thickening of the inner limiting membrane was stable and there was 1 asymptomatic preretinal hemorrhage inferotemporal to the macula (Figure 1C). The patient still experienced 5 to 6 episodes of migraine per year but was otherwise healthy.

In visual field tests, scotomas were noted that corresponded to the locations of the hemorrhages. Fluorescein angiography demonstrated no leakage, staining, hypoperfusion, or capillary dropout. Neurologic examinations, including cranial magnetic resonance imaging, yielded normal findings. Extensive examinations in internal medicine explicitly tests for serologic factors including virus and bacteria antibody titers and for rheumatologic and autoimmune factors, coagulation tests, and serum electrophoresis, also yielded normal findings. The patient was not taking any systemic medication that would alter coagulation, and blood pressure was within normal limits.

At nailfold capillaroscopy, which was performed at the second and fourth visits, tortuosity of capillaries was highly increased in all fingers of both hands (Figure 1D and E). Minor rarefication and 1 avascular zone but no microhemorrhages, were detected. Sodium fluorescein video nailfold capillaroscopy showed normal inflow and outflow demonstrating absence of capillary spasm; normal transcapillary and interstitial diffusion of fluorescein; and normal halo. No other dermatologic disease, including Raynaud syndrome, was observed.

Case 2. The older sister of patient 1 reported a slight decrease in BCVA when first seen at age 28 years. However, BCVA was 1.0 OU. We found marked tortuosity of second- and third-order retinal arteries in both eyes but no hemorrhages. The patient had a history of 1 episode of transient microhematuria of unknown origin, but otherwise reported that she was healthy.

Seven years later extensive ophthalmologic (**Figure 2**A), neurologic, and medical examinations were performed, analogous to those in patient 1. All findings were normal with the exception that antinuclear antibodies were 2-fold positive. Findings at dermatologic examination and nailfold capillaroscopy were identical to those in patient 1 (Figure 2B and C).

Case 3. The father of patients 1 and 2 was first seen at age 56 years and reported that he had never experienced any visual disturbances. He had a stroke with speech disturbance 8 years earlier, but reported no residual adverse effects. Best-corrected visual acuity was 1.0 OU. Marked tortuosity of second- and third-order retinal arteries was found in both eyes, without hemorrhages.

He was seen 7 years later and extensive ophthalmologic (**Figure 3**A), neurologic, and medical examinations revealed atrial fibrillation, and

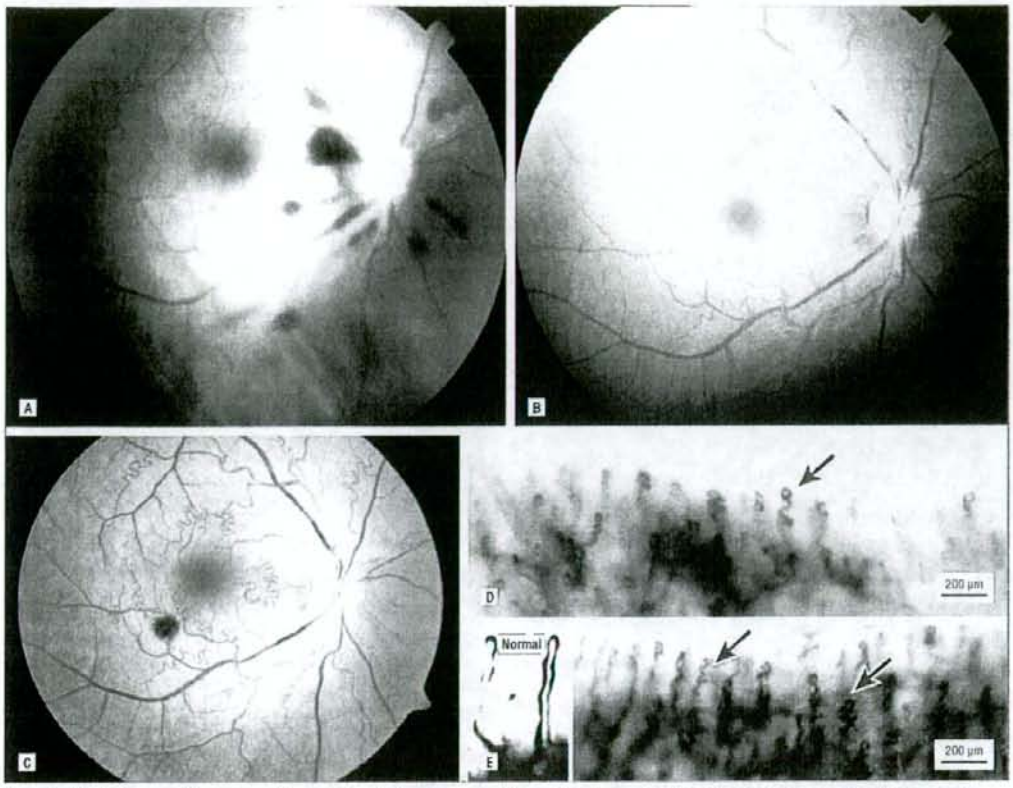

Figure 1. Patient 1. Views of the fundus and findings at nailfold capillaroscopy. A, When the patient was first seen after a minor car accident at age 19 years, multiple small hemorrhages were noted. She exhibited all of the typical features of familial retinal arterial tortuosity, with tortuosity in second- and third-order retinal arteries and normal large arteries and retinal veins. B, Five years later, no hemorrhages were seen and the retinal vasculature remained unchanged. C, Twelve years later, there was 1 preretinal hemorrhage inferotemporal to the macula; the retinal vasculature otherwise remained unchanged. D and E, Nailfold capillaroscopic findings in the right third and fourth fingers. Except for the high degree of tortuosity (present in approximately 30% of capillary loops; arrows depict typical examples), the capillaries were normal, a finding that was confirmed at sodium fluorescein video microscopy. For comparison, the inset in E shows enlargement of normal capillary loops at nailfold capillaroscopy in a healthy person. Note parallel arrangement of inflow and outflow arms.

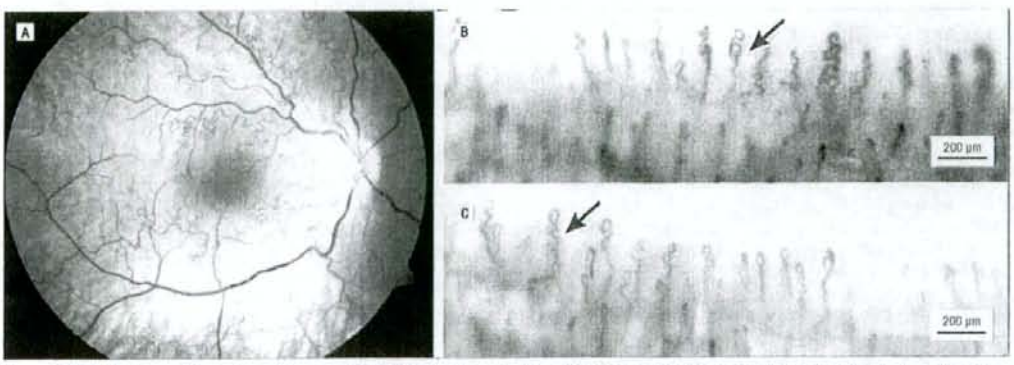

Figure 2. Patient 2. Views of the fundus and findings at nailfold capillaroscopy. A, At age 35 years, the patient demonstrated all of the typical findings of familial retinal arterial tortuosity. She had never experienced visual disturbances, although the degree of tortuosity was higher than in patient 1. B and C, Nailfold capillaroscopic findings in the left third and fourth fingers. Also in this patient, approximately 30% of capillary loops showed a high degree of tortuosity (arrows depict typical examples), while all other findings were normal, analogous to those in patient 1.

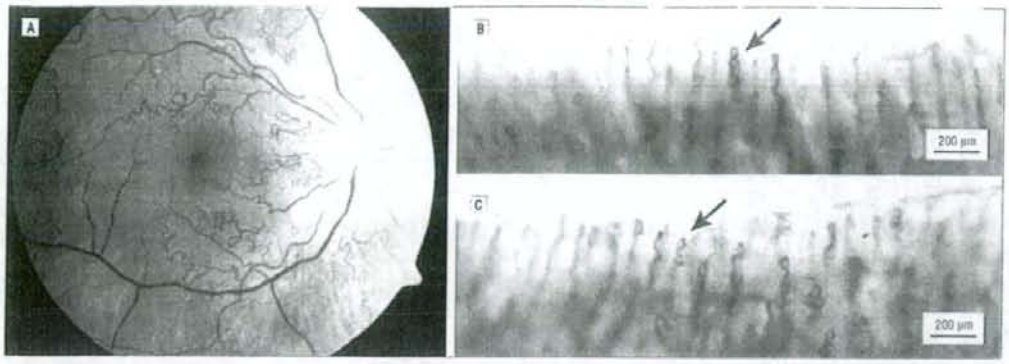

Figure 3. Patient 3. Views of the fundus and findings at nailfold capillaroscopy. A, When the patient was last seen at age 62 years, he demonstrated all of the typical findings of familial retinal arterial tortuosity. The patient had never experienced visual disturbances, although the degree of tortuosity was greater than in patients 1 and 2. B and C, Nailfold capillaroscopic findings in the patient's right second and fourth fingers. Approximately 30% of capillary loops showed a high degree of tortuosity (arrows depict typical examples), while all other findings were normal, analogous to those in patients 1 and 2.

warfarin sodium therapy was prescribed. As in patients 1 and 2, all other systemic findings were normal. Findngs at dermatologic examination and nailfold capillaroscopy were identical to those in patient 1 (Figure 2B and C).

Comment. All 3 patients had typical features of fRAT: only second- and third-order arteries were affected, while first-order arteries and the venous system were normal. The caliber, shape, and branchings of affected arteries were normal; no leakage or staining was observed at fluorescein angiography; symptomatic hemorrhages followed minor stress or trauma; visual prognosis was excellent; and no associated systemic disease was found in any of our 3 patients. These findings correspond well with the previously reported approximately 100 cases.[1,2] While in isolated cases systemic disease was found in patients with fRAT (malformation in the Kieselbach nasal septum, vascular mass in the spinal cord, sixth nerve palsy, simultaneous conjunctival hemorrhage, teleangiectasis of the bulbar conjunctiva), no consistent associated systemic disease has been reported and thus, fRAT was generally believed to be an isolated retinal finding.[2,3] Our finding of marked capillary tortuosity at nailfold capillaroscopy favors systemic vascular disease in fRAT.

Recently, a syndrome has been reported consisting of features of fRAT with hematuria, muscular contractures, and sporadic other disorders such as cardiac arrhythmia.[4] This syndrome is distinct from the finding in our patients; only patient 2 had transient microhematuria and pronounced tortuosity in nail bed capillaries, in contrast to the unspecific findings at nailfold capillaroscopy found in patients with the newly reported syndrome, which is dominated by renal disease.

Nailfold capillaroscopy, as it was performed in our patients, is considered a mirror of systemic vascular processes, and a high degree of validity of correspondence and prognostic value is found, for example, in diabetes mellitus, systemic scleroderma, primary chronic polyarthritis, and systemic lupus erythematosus, and especially with ocular capillaries and in glaucoma. Nailfold capillaroscopy demonstrated the identical features of capillary loops as retinal vessels in showing a high degree of tortuosity without any other pathologic findings such as leakage of dye, occlusion, or caliber abnormalities. A milder form of tortuosity at nailfold capillaroscopy has been described in patients with psoriatic arthritis,[5] but, to our knowledge, tortuosity of this magnitude has not been reported before. Considering that hemorrhages from retinal vessels are a hallmark of fRAT, manifestation in other tissues could be expected, although evidence for consistent systemic disease is thus far lacking in fRAT.

By demonstrating that capillary abnormalities are also found in nailfold capillaries of patients with fRAT, retinal vascular abnormalities can no longer be accepted as an isolated finding. We believe that, because of an increasing number of reports of this disease,[2] further investigation as to systemic involvement in patients with fRAT is warranted.

Florian Gekeler, MD
Kei Shinoda, MD, PhD
Michael Jünger, MD
Karl Ulrich Bartz-Schmidt, MD
Faik Gelisken, MD

Correspondence: Dr Gekeler, Department of Ophthalmology, University of Tübingen, Schleichstrasse 12-16, 72076 Tübingen, Germany (gekeler@uni-tuebingen.de).

Financial Disclosure: None reported.

Additional Information: This study conformed to the protocol of our institutional review board and did not require approval.

1. Goss DM. Macular dysfunction caused by retinal vascular diseases. In: Goss DM, ed. *Stereoscopic Atlas of Macular Diseases*. 4th ed. St Louis, Mo: Mosby-Year Book Inc; 1997.
2. Sutter FK, Helbig H. Familial retinal arteriolar tortuosity: a review. *Surv Ophthalmol*. 2003; 48:245-255.
3. Sears J, Gilman J, Sternberg P Jr. Inherited retinal arteriolar tortuosity with retinal hemorrhages. *Arch Ophthalmol*. 1998;116:1185-1188.
4. Plaisier E, Alamowitch S, Gribouval O, et al. Autosomal-dominant familial hematuria with retinal arteriolar tortuosity and contractures: a novel syndrome. *Kidney Int*. 2005;67:2354-2360.
5. Flammer J, Pache M, Resink T. Vasospasm, its role in the pathogenesis of diseases with particular reference to the eye. *Prog Retin Eye Res*. 2001;20:319-349.
6. Grassi W, Cervini C, Cortinovis G, Cervini C. Nailfold capillary permeability in psoriatic arthritis. *Scand J Rheumatol*. 1992;21:226-230.

Doc Ophthalmol (2006) 113:155–164
DOI 10.1007/s10633-006-9024-y

ORIGINAL PAPER

Phototoxic effects of commercial photographic flash lamp on rat eyes

Makoto Inoue · Kei Shinoda · Hisao Ohde · Keiji Tezuka · Tetsuo Hida

Received: 23 May 2006 / Published online: 3 October 2006

Abstract
Background To determine whether exposure of the cornea and retina of rats to flashes from a commercial photographic flash lamp is phototoxic.
Methods Sprague–Dawley rats were exposed to 10, 100, or 1,000 flashes of the OPTICAM 16M photographic flash lamp (Fujikoeki, Japan) placed 0.1, 1, or 3 m from the eyes. Corneal damage was assessed by a fluorescein staining score, and the retinal damage by eletroretinography (ERG) and histology before and 24 h after exposure.
Results Exposure of the eyes to 1,000 flashes at 0.1 m increased the fluorescein staining score significantly ($P = 0.009$, the Mann–Whitney test). Scanning electron microscopy (SEM) of the cornea showed a detachment of the epithelial cells from the surface after this exposure. The amplitude of the a-wave was decreased significantly by 23.0% ($P = 0.0026$) of the amplitude before the exposure, and the b-wave by 19.7% ($P = 0.0478$) following 1,000 flashes at 0.1 m but not by the other exposures. TUNEL-positive cells were present in the outer nuclear layer only after the extreme exposure, but no significant decrease in retinal thickness was seen under any condition. The fluorescein staining score and ERGs recovered to control levels within 1 week.
Conclusions Light exposure to a photographic flash lamp does not induce damage to the cornea and retina except when they are exposed to 1,000 flashes at 0.1 m.

Keywords Cornea · Electroretinograms · Photographic flash lamp · Phototoxicity · Retina

M. Inoue (✉) · K. Shinoda · H. Ohde
Department of Ophthalmology, Keio University School of Medicine, 35 Shinanomachi, Shinjuku, Tokyo 160-8582, Japan
e-mail: inoshin@sc.itc.keio.ac.jp

K. Shinoda
Laboratory of Visual Physiology, National Institute of Sensory Organs, National Organization Tokyo Medical Center, Tokyo, Japan

K. Tezuka
FUJIFILM Corporation, Tokyo, Japan

T. Hida
Kyorin Eye Center, Kyorin University School of Medicine, 6-20-2 Shinkawa, Mitaka, Tokyo 181-8611, Japan

Introduction

Human eyes are continuously exposed to sunlight and artificial lights, and excessive light exposure can induce tissue damage to different ocular structures. These changes have been studied both experimentally and clinically for photoreceptor damage by continuous low level

illumination, [1–3] corneal epithelial damage by ultraviolet (UV) irradiation, [4] retinal cell damage by light from an operating microscope or endoillumination during vitreous surgery, [5–8] and macular damage by a laser pointer [9]. Most of these injuries were caused by unnatural conditions, namely high intensities or long durations of the irradiation.

Commercially available photographic flash units for cameras were developed over a century ago so that photography could be performed under reduced light levels. They are generally considered to be safe because of their extremely short flash duration. However, the well-known after-images suggest that they do have a long-lasting effect on the retina, and the instruction manuals for the flash units warn users of the possibility of injury by firing the flash close to the eye. However, very few studies have been done to examine the phototoxicity of such flash units for cameras.

The aim of this study was to determine whether flashes from a commercially available photographic flash lamp can damage ocular tissues. The eyes of rats were exposed to different number of flashes from a commercially available photographic flash unit, and both morphological and physiological techniques were used to assess the cornea and retina.

Materials and methods

Animals and light exposure

All animals were cared for in accordance with the Statement by the Association of Research in Vision and Ophthalmology for the Use of Animals in Ophthalmic and Vision Research, and all research procedures were performed in compliance with the regulations on animal usage by Keio University, Tokyo, Japan.

Male Sprague–Dawley rats, weighing 150–200 g and 6- to 8-week-old, were anesthetized with an intramuscular injection of 100 mg/kg of ketamine and 10 mg/kg of xylazine. The right eyes were exposed to the photographic flash bulb (19196 OPTICAM 16M, Fujikoeki, Japan), but the left eyes were blocked from the light by an aluminum sheet and used for control. The flash bulb was placed 0.1, 1, or 3 m from the eye, and the number of flashes delivered was 10, 100, or 1,000 with an interflash interval of 5 s that was controlled by a personal computer (FMV, Fujitsu, Japan). During the exposures, rats were placed on a heating pad, and the body temperature was maintained at 36°C throughout the experiment. The corneas of both eyes were kept moist by frequent application of balanced salt solution and hydroxymethyl cellulose during and after the light exposure. A speculum was not used, but the eyes were kept widely opened to expose the light to the whole eye during the light exposure. Each rat was anesthetized for the same duration of 1.5 h, and supplemented by one-half of the original dose of ketamine and xylazine when the rat began to move. This duration of 1.5 h was equal to the maximal exposure of 1,000 times of flashes with an interval of 5 s. After the exposure to the flashes from the OPTICAM, the ocular surface was protected by application of an antibiotic ointment.

All animals were kept in the animal rooms for several days after they were received from the animal dealer. The luminance in the animal room at the cage level was 800 lux, and the lighting was set on a 12:12 h light:dark schedule. After animals were exposed to the flashes, they were returned to a darkened room because all experiments were done at night.

The photographic flash bulb (19196 OPTICAM 16M, Fujikoeki, Japan, color temperature 5,700 K; flash duration 0.5 ms) is a xenon bulb and emits light throughout the visible spectrum. A UV filter is incorporated in the unit to attenuate wavelengths below 380 nm. The spectral energy in a single flash of the xenon bulb ($n = 2$) was recorded with a spectroradiometer (USR-40V, Ushio Electronics, Japan) that was responsive to wavelengths 300–1,100 nm placed 5 cm from the flash unit.

Fluorescein staining score for corneal epithelial damage

Corneal epithelial damage was assessed by scoring the degree of fluorescein staining before, 24 h, and 7 days after the light exposure

Table 1 The experimental design and the numbers of the rats for the flash light exposure

Situation	Distance	Count	Fluorescein	ERG
Unusual	0.1 m	1,000	5	5
Usual	1 m	1,000	3	4
Usual	1 m	100	3	3
Usual	1 m	10	3	3
Usual	3 m	1,000	3	4
Usual	3 m	100	3	3
Usual	3 m	10	3	3
Control	No flash	0	3	3

Situation, the maximal exposure represents unusual accidental exposure. distance; the distance form the flash bulb to the rat eye, count; the numbers of flash light exposure, fluorescein; the numbers of the eyes examed in fluorescein score, ERG; the numbers of the eyes examed in electroretinograms. The three rats in condition of 1,000 flash at 0.1 m were sacrificed on the next day, but the rest of three rats were killed after 1 week

(Table 1). To do this, 10 μl of a 10% fluorescein solution was dropped on the cornea, and the excess dye was quickly washed out by balanced salt solution. The degree of fluorescein staining observed with a slit-lamp biomicroscope was scored from 0 to 3 with; 0 = no stain, 1 = slight stain with one spot of fluorescein, 2 = moderate stain with two or three spots of fluorescein, and 3 = severe stain with more than four spots of fluorescein (Fig. 1). The superior, central, and inferior regions of the cornea were scored separately, and the final score was the sum of these three regions with a range from 0 to 9. In addition, the degree of cataract was also evaluated by slit-lamp biomicroscopy.

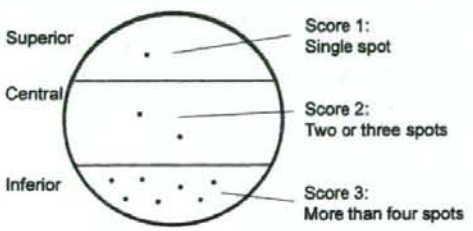

Fig. 1 Scoring of fluorescein score. The superior, central, and inferior regions of the cornea were scored separately, and the final score was the sum of these three regions with a range from 0 to 9

Electroretinography

Electroretinograms (ERGs) were recorded from both eyes simultaneously after more than 6 h of dark-adaptation before and 24 h after the light exposure (Table 1). ERGs were also recorded 7 days after the exposure to the maximum energy (1,000 flashes at 0.1 m). After anesthesia with an intramuscular injection of a mixture of ketamine (100 mg/kg) and xylazine (10 mg/kg), the pupils in both eyes were dilated with 10μl of 0.5% tropicamide and 0.5% of phenylephrine. The rats were placed on a heating pad, and the body temperature was maintained at 36°C throughout the experiment.

The cornea was anesthetized with topical benoxylchloride, and a contact lens electrode carrying white light-emitting diodes (LEDs; Kyoto Contact, Kyoto, Japan) was used to elicit and record the ERGs by a single flash of 10,000 cd-s/m^2 luminance in the dark with a stimulus duration of 5 ms. The reference electrode was a needle placed subcutaneously between the eyes, and another needle electrode was placed subcutaneously in the neck region as the ground electrode. Responses were differentially amplified and filtered with digital bandpass filters set at 0.5–200 Hz to record the a- and b-waves (Neuropack μ system, Nihon Koden, Tokyo, Japan). The amplitude of the a-wave or b-wave of the ERG of the affected right eye was compared to the amplitude of the same eye before light exposure and the amplitude ratios of after/before exposure of the ERG components were calculated.

Morphological evaluations

The animals were killed 24 h or a week after the light exposure by an intraperitoneal injection of sodium pentobarbital. The eyes were enucleated and the anterior segment was cut-off. The cornea was fixed in phosphate-buffered 2.5% glutaraldehyde and processed for scanning electron microscopy (SEM; S-4000, HITACHI, Japan). The eyecup was fixed in 4% paraformaldehyde overnight, embedded in paraffin, sectioned at 5μm, and stained with hematoxlyin and eosin for light microscopy. The superior

central and temporal retina has been described to be more susceptible than other areas [10, 11]. The thickness of outer nuclear layer (ONL) and sensory retina was measured from the histological section at approximately 1 mm temporal or superior to the optic disc with a width of 500μm in the experimental and control eyes ($n = 3$). The column cell count of the ONL nuclei (cell count) was also measured in the same histological sections.

To detect apoptotic cells, the terminal deoxynucleotidyl transferase (TdT)-mediated, dUTP-biotin catalyzed DNA nick-end labeling (TUNEL) method was used (In situ apoptosis detection kit, Takara, Japan). The TUNEL enzyme (1 h at 37°C) and peroxidase converter (30 min at 37°C) were applied to the sections after the sections were incubated in a permeabilizing solution of 0.1%Triton-X in 0.1% sodium citrate for 2 min on ice. DAB was used as the chromogen. TUNEL-positive cells were counted in the ONL or inner nuclear layer (INL) from the same area of the histological sections.

Statistical analyses

Mann–Whitney U test was used to compare fluorescein staining scores between the exposed eye and control eye. The significance of differences in the amplitude ratio of ERG components between groups was evaluated by the one-factor ANOVA followed by Scheffe's F test. Fisher's least significant difference (LSD) test was performed to determine if the differences in the mean thickness of the outer nuclear layers between affected and control eyes were statistically significant. The differences were considered significant when $P < 0.05$.

Results

Spectral emission of flash unit

The spectral energy output from the photographic light bulb was measured with the spectroradiometer and plotted in Fig. 2. Emissions at wavelengths less than 380 nm were reduced significantly by the UV filter incorporated in the unit. However, a small amount of UV between 380 nm and 400 nm was transmitted through the filter, and a large amount of near-infrared radiant was emitted by the photographic flash lamp. The intensity of the light bulb was calculated to be 40 ± 2 J/m^2 ($n = 2$).

Fluorescein staining score

The mean ± standard deviation of the fluorescein score following the maximal light exposure

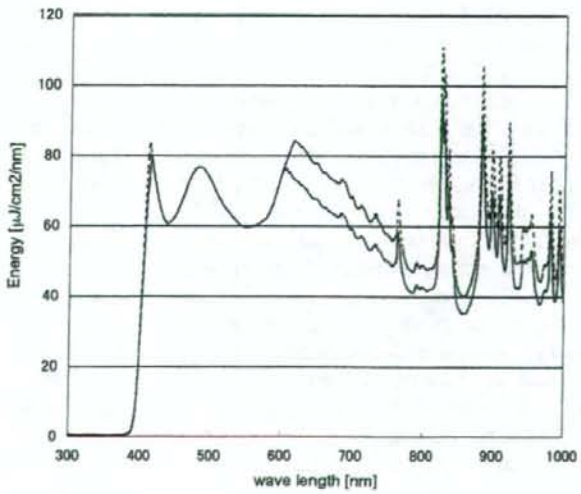

Fig. 2 Spectral emission of the light bulb. This bulb emits light throughout the visible spectrum and a UV filter is incorporated in the unit to attenuate wavelengths shorter than 380 nm

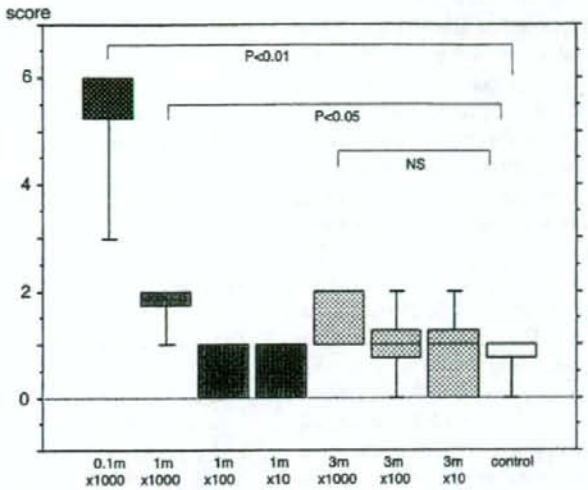

Fig. 3 Fluorescein staining score of the corneal epithelium 24 h after light exposure. The fluorescein scores after the maximum light exposure conditions (1,000 flashes at 0.1 m) and the exposure (1,000 flashes at 1 m) are significant higher than that of controls ($P = 0.009$, $P = 0.028$, the Mann–Whitney U test, respectively). Other exposures are not significantly different from that of controls (NS: not significant, box: Median ± 25 percentile, bar: range of actual measurement)

(1,000 flashes at 0.1 m) was 5.4 ± 0.9, which was significantly higher than that of control eyes (0.8 ± 0.4; $P = 0.009$, the Mann–Whitney U test, Fig. 3). The fluorescein scores for eyes set at 1 m (1.8 ± 0.4; $P = 0.028$, the Mann–Whitney U test) was also significantly higher but that at 3 m (1.6 ± 0.5; $P = 0.076$, the Mann–Whitney U test) was not significantly different from the scores of the control eyes. The fluorescein scores for eyes set at 1 m were 0.4 ± 0.5 after 10 flashes, and 0.6 ± 0.5 after 100 flashes, and the scores for eyes set at 3 m were 0.8 ± 0.8 after 10 flashes, 1.0 ± 0.7 after 100 flashes, and 1.6 ± 0.5 after 1,000 flashes. The fluorescein score increased as the number of flashes increased, but the increases in the scores were not significantly different from that of the control eyes.

The fluorescein score 7 days after the maximum light exposure (1,000 flashes at 0.1 m) had decreased to the control level of 0.6 ± 0.5 indicating a recovery of the corneal epithelium ($n = 2$). No cataract was seen by slit-lamp examination before and after any light exposure conditions.

Scanning electron microscopy (SEM)

Examinations of the corneas obtained after exposure to the maximum light conditions (1,000 flashes at 0.1 m) by SEM showed that many of the epithelial cells were detached from the surface of the cornea (Fig. 4). With less than 1,000 flashes or at farther distances of 3 m, no such changes were detected, and the hexagonal shapes of epithelial cells were well-preserved. The corneal epithelium recovered to the control level 7 days after the maximum light exposure (1,000 flashes at 0.1 m, $n = 2$).

Electroretinography (ERG)

The amplitude ratios (of after/before the light exposure) of the a-wave and b-wave were significant between groups ($P = 0.0006$, $P = 0.0384$, one factor ANOVA test, Figs. 5 and 6). In the eyes exposed to the maximum light level (1,000 flashes at 0.1 m), the mean ± standard deviation of the amplitude of the a-wave was significantly reduced by 23.0 ± 10.7% ($P = 0.0026$,

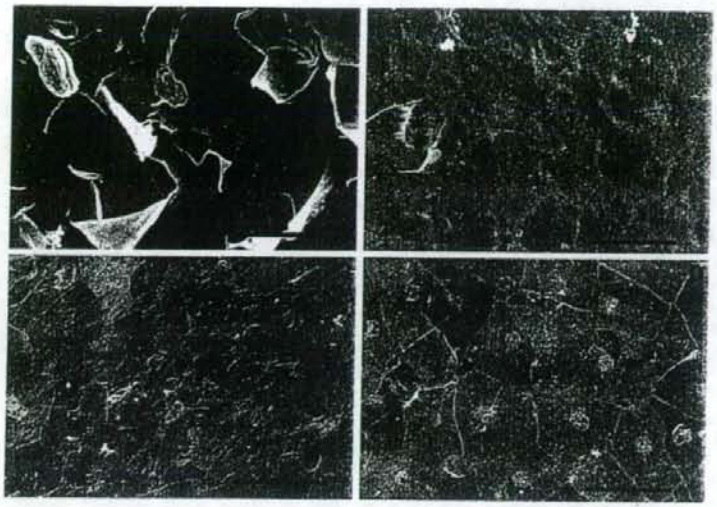

Fig. 4 Scanning electron photographs of cornea 24 h after light exposure. A: 1,000 flashes at 0.1 m. Edges of epithelial cells are detached from the surface of the cornea. B: 1,000 flashes at 1 m. No changes are seen. C: 1,000 flashes at 3 m. No changes are seen. D: control. No difference is observed at the longer distances (1 m or 3 m) even with the maximal number of flashes compared to the control (bar: 45 μm)

the Scheffe's F test) of that before the light exposure, but the amplitude in the eyes exposed at longer distances of 1 m or 3 m to 1,000 flashes was not reduced significantly (Figs. 5, 6A, $P > 0.9999$, $P = 0.9656$, respectively, the Scheffe's F test). The amplitude of the b-wave exposed to the maximum light level (1,000 flashes at 0.1 m) was also significantly reduced by 19.7 ± 7.0% (Figs. 5, 6B, $P = 0.0478$, the Scheffe's F test) of that before light exposure, but the amplitude in the eyes exposed at farther distances of 1 m or 3 m was not significantly reduced ($P = 0.8821$, $P = 0.6561$, respectively, the Scheffe's F test). The amplitude ratio of the control left eyes (no light exposure) was 100.4 ± 5.1% for the a-wave and 100.5 ± 6.7% for the b-wave. The amplitudes in a- and b-waves were not altered significantly following the other exposure levels.

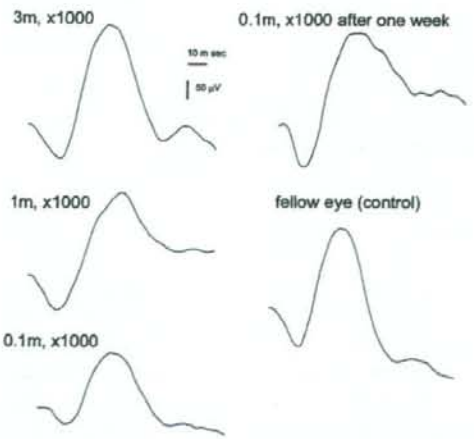

Fig. 5 Electroretinograms (ERGs) of rat eyes 24 h after the light exposure. The amplitudes of the a- and b-waves are reduced after the maximal light exposure (1,000 flashes at 0.1 m) but the amplitudes recover after 1 week

The amplitude of ERG components in the eyes exposed to the maximum light level recovered to 100.6 ± 13.3% for the a-wave and 100.8 ± 2.9% for the b-wave 1 week after the light exposure ($n = 2$).

Histopathological examination of retina

The mean thickness of the outer nuclear layers temporal and superior to the optic disc was 24 ± 1μm at 0.1 m with 1,000 flashes, 24 ± 2 μm at 1 m, 25 ± 2μm at 3 m and 24 ± 1μm in controls without light flashes (Fig. 7). These differences were not significant ($P = 0.92$ at 0.1 m, $P = 0.40$ at 1 m, $P = 0.45$ at 3 m, the LSD test). The architecture of the retina was not altered by any exposed level. The mean retinal thickness in the same area of the control eyes was 83 ± 6 μm, and the thickness in the same area was 86 ± 11 μm when the flash unit was set at 0.1 m and 1,000

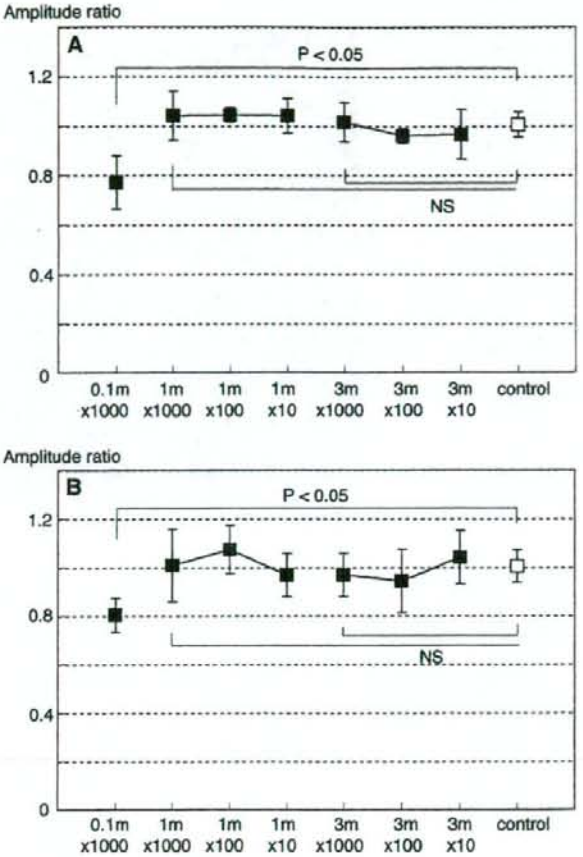

Fig. 6 The amplitude of the electroretinogram (ERG) of rat eyes 24 h after the light exposure. A: The amplitude of a-wave of the ERG following the maximum light exposure (1,000 flashes at 0.1 m) is reduced by 23.0% ± 10.7% ($P = 0.0026$, the Scheffe's F test) from the amplitude before the light exposure. No significant changes are seen following other levels of exposures. B: The amplitude of b-wave of the ERG following the maximum light exposure (1,000 flashes at 0.1 m) is reduced by 19.7% ± 7.0% ($P = 0.0478$, the Scheffe's F test) from the amplitude before the light exposure. No significant changes are seen following other levels of exposures (Amplitude ratio: the ratio of amplitude after the light exposure comparing before the exposure, NS: not significant, bar; mean ± standard deviation)

flashes were delivered. This difference was also not significant comparing with the control eyes ($P = 0.287$, the LSD test). Lower levels of light exposures also did not change the retinal thickness significantly (85 ± 7 μm at 1 m, $P = 0.591$, and 86 ± 14 μm at 3 m with 1,000 flashes, $P = 0.116$, the LSD test).

A significantly larger numbers of TUNEL positive cells were observed in the ONL of eyes exposed to the maximal light exposure (Fig. 8, $P = 0.02$, the LSD test). The ratio of the TUNEL positive cells to total cells was 0.52 ± 0.39% in the ONL in the eyes which had the maximal light exposure, while it was 0.03 ± 0.01% in the INL. With other light exposure conditions, none of the eyes showed more than 0.03% TUNEL positive cells in the ONL and the INL. No TUNEL positive cells were observed 1 week after the maximal light exposure.

Discussion

Damage of the ocular tissues in albino rats was produced only by the maximum exposure of the photoflash unit. This exposure exceeded that encountered in typical use of a flash photography unit. In addition, the damage was reversible. Excessive light exposure of the eye is known to damage the cornea, crystalline lens, retina, and retinal pigment epithelial cells [2, 3]. In the cornea, the damage is mainly of the epithelial cells which

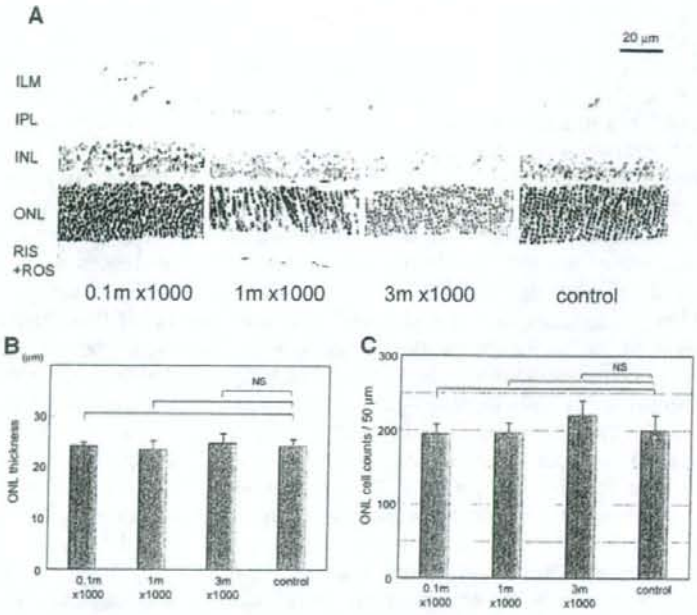

Fig. 7 Paraffin sections of posterior pole of the eyes 24 h after light exposure. A: Histological sections of posterior pole indicate no morphological damage in the retina of the eye for all levels of light exposure compared to the control eyes (Hematoxylin & eosin stain). B: The total retina thickness and C: the thickness of outer nuclear layer (ONL) 24 h after 1,000 flashes in each distance are not significant to those of control eyes

are detached from the surface of the cornea, and this change is caused by the light from the UV-end of the spectrum [4]. Although the flash unit used in this experiment is equipped with a UV filter that greatly attenuates wavelengths shorter than 380 nm, our findings showed that sufficient UV energy was still transmitted to the cornea to cause the detachment of some of the epithelial cells.

Chronic light exposure can lead to photochemical alterations to the lens which also results from the absorption of UV-A light to cause nuclear cataracts [2]. Intensive laser irradiation can cause heat-derived lens opacification in the patients with cataracts, but visible light, such as that emitted from photographic flash units for a short duration is unlikely to cause serious damage to the crystalline lens.

Light damage to the retina has been shown to result from either thermal or photochemical effects. From the studies of Noell and colleagues, the photochemical effect is most likely the major factor involved in the retinal light damage [12].

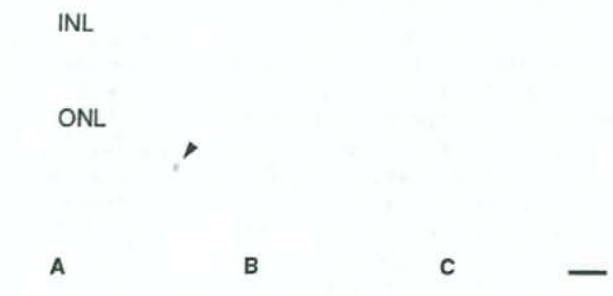

Fig. 8 Apoptosis following light exposure in the posterior pole of the eyes 24 h after light exposure. A: 0.1 m × 1,000 flashes. B: 1 m × 1,000 flashes. C: 3 m × 1,000 flashes. TUNEL-positive cells (arrow head) are seen in outer nuclear layer (ONL), indicating apoptosis of the photoreceptorcells following the maximal exposure but no positive cells in other conditions (bar: 20 μm)

The thermal effects result from an increase in temperature caused by the absorption of light energy by the melanin pigments in the RPE and choriod [12]. Blue light irradiation, on the other hand, leads to a minimal increase in temperature, but the threshold of blue light energy necessary to cause tissue damage was estimated to be <0.001 of that of infrared irradiance [13]. Thus, these characteristics indicate that the photochemical effect played a major role in the retinal damage caused by visible light.

The mechanism for the damage has been suggested to arise from the production of phototoxic substances by the partially transmitted UV-light or blue light from the flash lamp. On the other hand, high tissue temperatures can enhance tissue damage and low temperatures minimize the damage [14, 15]. Thus, the near-infrared radiant component in the photographic flash light may enhance tissue damage. However, the synthesis of heat-shock proteins induced by a brief, whole body hyperthermic treatment has been shown to be protective by enhancing photoreceptor cell survival against light damage [16, 17].

Reductions in the amplitude of the ERGs has been reported to indicate retinal light damage and is correlated with the degree of retinal damage [18–22]. Our results showed that the ERGs recorded from the eyes exposed to the maximum light levels were reduced at 24 h after exposure, but they recovered to normal values after 1 week. These transient decreases of ERG amplitude may reflect physiologically a consumption of the outer segments of the photoreceptors without significant histological degeneration of the ONL and the outer segments may have been renewed within a week.

Retinal light damage has also been investigated histologically [22–25]. Blue light damage was reported to cause depigmentation of the retinal pigment epithelium, while near UV light caused tissue damage in the outer segments in addition to the RPE damage [25]. These wavelengths are thought to induce oxidative stress after their absorption in the tissue [26, 27]. In our study, histological examinations did not reveal any major damage in retinal architecture with no significant change in retinal thickness. However, a significant increase in the number of TUNEL-positive apoptotic nuclei was observed in the outer nuclear layer after the maximal light exposure. TUNEL positive cells have been reported to be present in the outer nuclear layer after photic injury to the rat retina [28, 29]. Intense light exposure can induce apoptotic changes in many photoreceptor cells even after a short exposure, and this would suggest that the photoreceptor cell death starts immediately after the exposure [29]. However, the percentage of TUNEL-positive apoptotic cells were only 0.52% even after the maximal exposure which should then not affect the total retinal cell structure to decrease the retinal thickness in the ONL.

Our results showed that the light exposure of the photographic flash unit can cause transient corneal epithelial cell damage and transient impairment in retinal function. It is suggested that the threshold for corneal and retinal damage may lie between the maximum exposure and the next highest. However, this maximal exposure condition is very unusual. An exposure of 1,000 flashes at 0.1 m corresponds to approximate 100,000 flashes at 1 m in total light energy if the distance of 1 m can be considered to be the one used in normal situations. Therefore, we conclude that the phototoxic effect of this commercially available photographic flash unit is minimal to the cornea and retina when used in an appropriate way.

Acknowledgements This study was supported by the research grant by Fuji Film Corporation, Tokyo, Japan. The authors would like to acknowledge the technical assistance of T. Nagai with electron microscopy.

References

1. Wasowicz M, Morice C, Ferrari P, et al (2002) Long-term effects of light damage on the retina of albino and pigmented rats. Invest Ophthalmol Vis Sci 43:813–820
2. Zrenner E (1990) Light-induced damage to the eye. Fortschr Ophthalmol 87(suppl):S41–S51
3. Roberts JE (2001) Ocular phototoxicity. J Photochem Photobiol B 64:136–143
4. Podskochy A, Gan L, Fagerholm P (2000) Apoptosis in UV-exposed rabbit corneas. Cornea 19:99–103
5. Jaffe GJ, Irvine AR, Wood IS, et al (1988) Retinal phototoxicity from the operating microscope. The role of inspired oxygen. Ophthalmology 95:1130–1141